

# The large diameter and fast growth of self-organized TiO<sub>2</sub> nanotube arrays achieved via electrochemical anodization

H Yin, H Liu and W Z Shen<sup>1</sup>

Laboratory of Condensed Matter Spectroscopy and Opto-Electronic Physics, Department of Physics, and Institute of Solar Energy, Shanghai Jiao Tong University, 1954 Hua Shan Road, Shanghai 200030, People's Republic of China

E-mail: [wzshen@sjtu.edu.cn](mailto:wzshen@sjtu.edu.cn)

Received 12 September 2009, in final form 12 November 2009

Published 7 December 2009

Online at [stacks.iop.org/Nano/21/035601](http://stacks.iop.org/Nano/21/035601)

## Abstract

We have carried out a detailed investigation of the effect of water content on the electrochemical anodization of Ti in electrolytes consisting of ammonium fluoride, water, and ethylene glycol. We have explored the possible growth of ordered TiO<sub>2</sub> nanotubes in the electrolyte with water concentrations from 1 to 100 vol% and the applied voltage from 10 to 150 V, where large diameter ( $\sim 600$  nm) and fast growth rate ( $\sim 100 \mu\text{m h}^{-1}$ ) have been successfully realized for the self-organized TiO<sub>2</sub> nanotube arrays. The achievement benefits from the clear understanding of the effects of both the water content and the anodization voltage on the formation of TiO<sub>2</sub> nanotube arrays. We have further shown crystalline formation of TiO<sub>2</sub> nanotubes by simple thermal annealing. The mechanisms of the effect of the water content on the diameter and growth rate revealed here should establish a basis for further optimization of the TiO<sub>2</sub> nanotube geometries.

(Some figures in this article are in colour only in the electronic version)

## 1. Introduction

TiO<sub>2</sub> nanotubes have attracted tremendous attention due to the combination of a wide band gap semiconductive nature with high surface area and high aspect ratio. Their excellent optical and electrical characteristics make them suitable for use in water splitting [1], dye-sensitized solar cells (DSSCs) [2, 3], and photocatalysis [4]. Due to the specific ion intercalation properties, TiO<sub>2</sub> nanotubes can also be used in electrochromic display devices [5]. Their biocompatibility further makes them important for biomedicine application [6]. For fabricating TiO<sub>2</sub> nanotubes, a great many approaches, such as template-based, hydrothermal, and sol-gel methods, have been exploited [7–9]. Recently, self-organized growth by anodization has drawn much more attention [10–13]; this has the advantages of simplicity and of vacuum and high temperature being unnecessary, while retaining quite regular ordering. In the self-organized growth, each individual TiO<sub>2</sub> nanotube is perpendicular to the membrane surface and the TiO<sub>2</sub> layer has a good ohmic contact with the Ti substrate.

Since the first report on anodic TiO<sub>2</sub> nanotubes by Zwilling *et al* in 1999 [14], more and more studies have been followed up. Among those studies, the tube formation, including the tube morphology and controlling of tube sizes (diameter and length), has become an interesting topic, and is the basis for further investigation of the optical and electrical properties and related applications. The electrochemical system plays a key role in the optimized growth. Three generations of fluorine-containing electrolytes have been employed for anodization of Ti foil to fabricate TiO<sub>2</sub> nanotube arrays. The first-generation electrolyte is based on dilute hydrofluoride (HF) acid aqueous solution, in which the maximum thickness of TiO<sub>2</sub> nanotube arrays is limited to just several hundred nanometers due to the high rate of chemical dissolution of TiO<sub>2</sub> by fluorine ions [15, 16]. The second-generation electrolyte, a fluorine-containing buffer solution, can achieve arrays of TiO<sub>2</sub> nanotubes several micrometers in length by controlling the PH gradient within the growing nanotube to reduce the dissolution [11, 17]. At present, the third-generation electrolyte which consists of fluoride and a viscous organic electrolyte such as ethylene glycol (EG)

<sup>1</sup> Author to whom any correspondence should be addressed.

or glycerol is prevalent applications, and can produce TiO<sub>2</sub> nanotube arrays with an ultrahigh aspect ratio [13, 18–21]. Up to now, the largest tube diameter (in this paper, ‘tube diameter’ stands for the outer diameter), the longest tube length, and the fastest growth rate have been reported to be 300 nm [22], 1000 μm (in nine days) [23], and 60 μm h<sup>-1</sup> [24], respectively, for the third-generation electrolyte.

In this paper, we report the realization of tunable TiO<sub>2</sub> nanotubes with the largest diameter of 600 nm and the fastest growth rate of about 100 μm h<sup>-1</sup> in an electrolyte of water and EG with a little addition of NH<sub>4</sub>F. The success lies in the clear understanding of the effects of both the water content and the anodization voltage on the formation of TiO<sub>2</sub> nanotube arrays with systematic change of the applied voltage and water content from 1 to 100 vol%. This work was motivated by the fact that TiO<sub>2</sub> nanotube formation consists of two major processes: electrochemical oxidization and chemical dissolution of the oxide by F<sup>-</sup> ions through  $\text{Ti} + 2\text{H}_2\text{O} \rightarrow \text{TiO}_2 + 4\text{H}^+ + 4\text{e}^-$  and  $\text{TiO}_2 + 4\text{H}^+ + 6\text{F}^- \rightarrow \text{TiF}_6^{2-} + 2\text{H}_2\text{O}$ , where addition of water will affect both the ionization of NH<sub>4</sub>F and the mobility of the F<sup>-</sup>, O<sup>2-</sup>, and TiF<sub>6</sub><sup>2-</sup> species. TiO<sub>2</sub> tubes with larger tube size can have greater super-hydrophilic and super-hydrophobic behavior before and after treatment with octadecylphosphonic acid, respectively, which may be very useful in various fields, such as cell adhesion or protein adsorption [25], and a larger tube diameter allows a larger range of amounts and eluting rates controlled in drug elution [26].

## 2. Experimental details

Prior to the anodization, the Ti foils (0.25 mm thick, 99.7% purity, Sigma-Aldrich) used in this study were cleaned via ultrasonic baths in acetone, isopropanol, methanol, and ethanol, respectively, followed by subsequent rinsing in de-ionized water and drying with nitrogen. Electrochemical anodization of the Ti foils was performed in a two-electrode configuration using a direct current power supply (Agilent 5720), in which a Cu sheet was used as the counter electrode, and a Keithley 2400 sourcemeter was used to measure the resulted current. Anodizing was undertaken in a quiescent solution of 0.09 M NH<sub>4</sub>F in de-ionized water and EG. The water concentration in the solution was 1, 5, 10, 20, 30, 50, 70, 90, and 100 vol% and the experimental voltage ranged from 10 to 150 V. All electrolytes were prepared from reagent grade chemicals. NH<sub>4</sub>F acts as a pore opening reagent and the NH<sub>4</sub>F concentration also plays a key role in controlling the surface morphology, but we fixed it into 0.09 M in order to focus on the effects of the water concentration and applied voltage. For the balance of the ordering (which requires low temperature) and the growth rate (which requires higher temperature), we have fixed the temperature at a moderate value of 20 °C. The anodization includes an initial voltage ramp before reaching a certain value, and afterward a constant voltage fixed for 1 h.

The TiO<sub>2</sub> nanotube arrays yielded were rinsed with de-ionized water and dried in air spontaneously after the experiments. Their morphology and structure were characterized by a field-emission scanning electron microscope

(FE-SEM; Philips XL30FEG) with an accelerating voltage of 5 kV. In order to produce defined anatase structure, all the samples were annealed at 500 °C for 10 min in air with a heating rate of 10 °C min<sup>-1</sup> by using a muffle furnace (Thermo Scientific F48020). Raman measurements were carried out to examine the crystalline form of both as-prepared and annealed TiO<sub>2</sub> nanotube arrays at room temperature using a Jobin Yvon LabRAM HR 800UV micro-Raman system. The Raman spectra were recorded in a backscattering configuration using an exciting wavelength of 514.5 nm from an Ar<sup>+</sup> laser.

## 3. Results and discussion

### 3.1. Tuning of the TiO<sub>2</sub> nanotube diameter

In order to investigate the influence of the water content in the organic electrolyte, we have carried out preliminary experiments with electrolytes containing 0.09 M NH<sub>4</sub>F and a mixture of water and EG with volume ratios from 1:99 to 100:0 vol%. Taking the applied anodization voltage of 30 V as an example, where TiO<sub>2</sub> nanotubes can be formed over almost the whole range of water concentration, our experiments show that the average diameter increases from 85 to 180 nm as the water content goes from 1 to 50 vol%, and then decreases back to 120 nm when it goes up to 70 vol%. Figures 1(a–a'') present the top-view SEM micrographs of TiO<sub>2</sub> nanotube arrays obtained by Ti anodization at 30 V in different electrolytes containing 0.09 M NH<sub>4</sub>F and a mixture of water and EG with three volume ratios: (a) 10:90, (a') 30:70, and (a'') 50:50 vol%, for which the tube diameter is 110, 140, and 180 nm, respectively. This is evidence supporting the above result. Another phenomenon is that the nanostructure becomes less ordered with water content increasing, i.e., the standard deviation of the diameters is larger. Considering the relationship among the diameter, uniformity, and water content, TiO<sub>2</sub> tubes with both larger diameter and higher order, which may benefit the applications in cell adhesion, protein adsorption [25], and drug elution [26], should be obtained in electrolyte containing H<sub>2</sub>O less than 50 vol%.

We have further studied the dependence of the TiO<sub>2</sub> nanotube diameter on the anodization voltage exerted in 0.09 M NH<sub>4</sub>F in EG with different water contents. We have found that the greater the water content is, the smaller the anodization voltage range in which ordered tubes can be formed is. For instance, we can achieve ordered nanotube arrays in electrolyte containing 0.09 M NH<sub>4</sub>F and a mixture of water and EG with 1:99 vol% between 30 and 150 V, in which the corresponding diameters are from 85 to 300 nm. When the applied potential exceeds the range, there are only disordered porous nanostructures or a compact oxide layer left. As the ratio of water/EG changes to 90:10 vol%, the anodization voltage range reduces to just between 10 and 25 V. Figures 1(b–b'') show the cross-sectional SEM micrographs of anodic TiO<sub>2</sub> nanotube arrays in electrolyte containing 10 vol% H<sub>2</sub>O for 1 h at different applied potentials: (b) 60, (b') 110, and (b'') 140 V. Their average diameters are 200, 300, and 450 nm, respectively. Moreover, our detailed SEM observations for a series of applied voltages indicate that the average tube

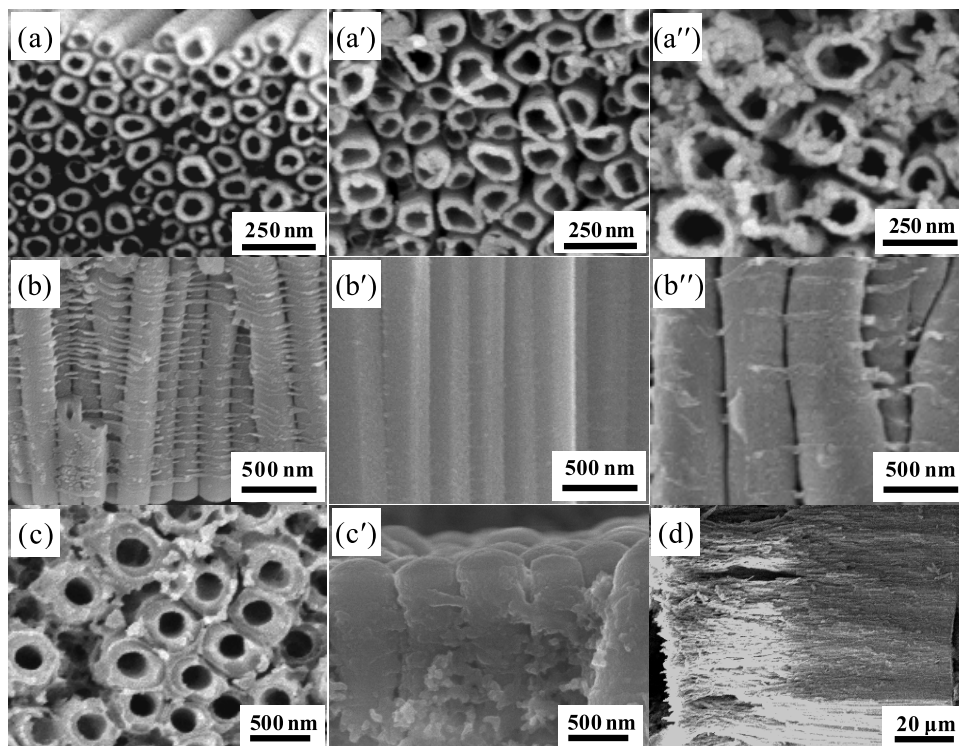


**Figure 1.** SEM images of TiO<sub>2</sub> nanotube arrays obtained from Ti anodization in 0.09 M NH<sub>4</sub>F in EG, with water contents of: (a) 10 vol%, (a') 30 vol%, and (a'') 50 vol% H<sub>2</sub>O at 30 V; 10 vol% H<sub>2</sub>O at (b) 60 V, (b') 110 V, and (b'') 140 V. SEM (c) top and (c') cross-sectional views of the giant TiO<sub>2</sub> tubes with diameters of about 600 nm under 10 vol% H<sub>2</sub>O at 150 V; and (d) an SEM cross-sectional view of the fast growth rate ( $\sim 100 \mu\text{m h}^{-1}$ ) of TiO<sub>2</sub> tubes under 1 vol% H<sub>2</sub>O at 150 V.

diameter is linearly proportional to the anodization voltage in every fixed water concentration, which is also supported by our other experiments with two alternative anodization voltages. Whether the voltage jumped up or down between the two voltages, an apparent interface can be clearly observed between the two nanotube layers with different diameters corresponding to the different voltages.

We have illustrated in figure 2 all the potential ranges under the different water contents for which ordered TiO<sub>2</sub> nanotube arrays can be formed. It is clear that figure 2 presents rich information on the tube diameter which covers H<sub>2</sub>O concentration from 1 to 100 vol% and anodization voltage from 10 to 150 V. As we know, the diameter of the TiO<sub>2</sub> nanotube arrays becomes larger and larger along with the water content going from 1 to 50 vol% and the voltage soaring. As a result, it is possible to grow self-organized TiO<sub>2</sub> nanotube arrays with large diameters of up to 600 nm just by optimizing the water content and anodization voltage. On one hand, when the water content is more than 20 vol%, the maximum diameter of the tube is less than 300 nm, since the voltage range in which ordered tubes can be formed is drastically reduced. On the other hand, when the water content is less than 1 vol%, the formation of large tubes ( $>300$  nm) is also impossible no matter what voltage is employed. Therefore, for the fabrication of large tubes ( $>300$  nm), addition of water content between 1 and 20 vol% is anticipated. We have successfully fabricated large diameter TiO<sub>2</sub> nanotube arrays ( $\sim 600$  nm) by tuning the water content and the voltage, as shown in figures 1(c, c'), in 0.09 M NH<sub>4</sub>F in EG with 10 vol% water at 150 V.

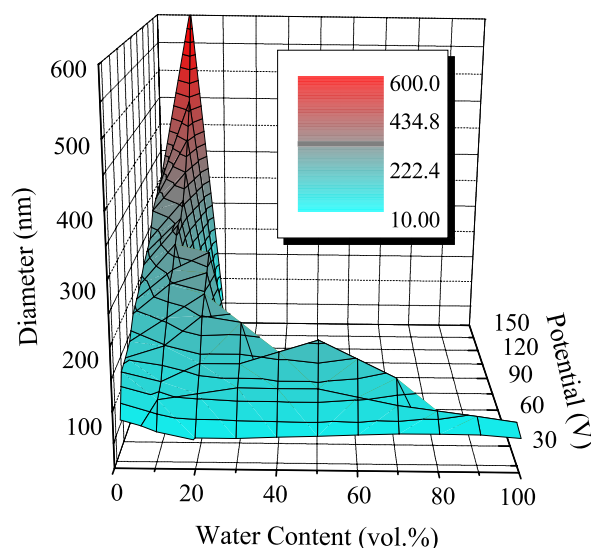


**Figure 2.** Diameters of different TiO<sub>2</sub> nanotube arrays achieved in 0.09 M NH<sub>4</sub>F in EG, with different water contents (from 1 to 100 vol%) and different voltages (from 10 to 150 V). All of the samples were fabricated at 20 °C for 1 h.

### 3.2. Mechanism of the effect of water on the tube diameter

The effect of the water content on the tube diameter might be explained as follows. In the anodizing process, TiO<sub>2</sub> nanotube arrays were self-organized through the delicate dynamic

balance of electric field induced oxidation of Ti and the chemical dissolution of  $\text{TiO}_2$  by  $\text{H}^+$  and  $\text{F}^-$  under an electric field [27]. We assume two factors prior to the discussion of the mechanism: (i) according to the Stokes–Einstein relation, the diffusion coefficient is inversely proportional to the viscosity of the solution; the diffusion of  $\text{H}^+$  and  $\text{F}^-$  is expected to be enhanced with the water concentration increasing; and (ii) during the anodization, the oxidation rate is significantly inhibited by the thickness of the barrier layer, i.e., as the barrier layer grows, the oxidation rate decreases until it is finally equal to the dissolution one. When the barrier layer gets thinner, the oxidation rate increases, until a final balance with the dissolution rate is established.

As shown in figure 3(a), when the water concentration increases from 1 to 50 vol%, at the initial anodizing stage, the dissolution rate at the tip of the tube bottom increases but is still lower than the oxidation rate, and the barrier layer has enough time to reach the maximum thickness,  $r_{\text{max}}$ , which is directly proportional to the anodization voltage [27]. With the increase of the dissolution rate, the diameter of the semicircular tip of the tube bottom becomes larger and larger, and the thickness of the barrier layer is still constant, which results in increase of the tube diameter. Besides, at a fixed anodization voltage, the voltage drop across the whole Ti foil increases with the water content also due to the reduced resistance of the electrolyte, which leads to an additional increase  $\delta r$  from  $r_{\text{max}}$ . Therefore, the tube diameter increases monotonically with the increasing water content range, from 1 to 50 vol%. However, when the water concentration goes beyond 50 vol%, the dissolution rate exceeds that of oxidation and the chemical dissolution becomes the dominant reaction. As the barrier layer expands to  $r_1$  (smaller than the maximum layer thickness in that condition), the tip has reached full depth and the tube at that position has no chance to expand further, since the oxidation only takes place near the bottom of the tube. As a consequence, the tube diameter decreases even though the voltage drop across the Ti foil still rises slowly.

Furthermore, the voltage range in which ordered  $\text{TiO}_2$  tubes can be formed becomes narrow in electrolytes with increasing water content (see figure 2). On one hand, if the applied voltage is too low, the electric force has so small an influence on the  $\text{F}^-$  ion that the dissolution in the vertical direction into the depth of the bulk Ti can hardly happen—where the tube formation cannot be initialized and there is only a compact oxide layer on the surface; the low voltage limit slowly decreases with increasing water content since the dissolution in the vertical direction is accelerated because of more highly concentrated  $\text{F}^-$  ions due to stronger ionization and higher mobility due to lower viscosity. On the other hand, when the applied voltage is too high, the distortion of the field at the top of the tube makes the dissolution in the other directions greatly accelerated by the component of the electric field. Soon after the oxide layer is formed, dissolution happens from many directions, which again encourages distortion of the electric field. This process results in a very disordered porous form of  $\text{TiO}_2$  tubes. With increasing water content, the upper voltage limit decreases significantly as a result of the enhancement of the multi-direction dissolution process at

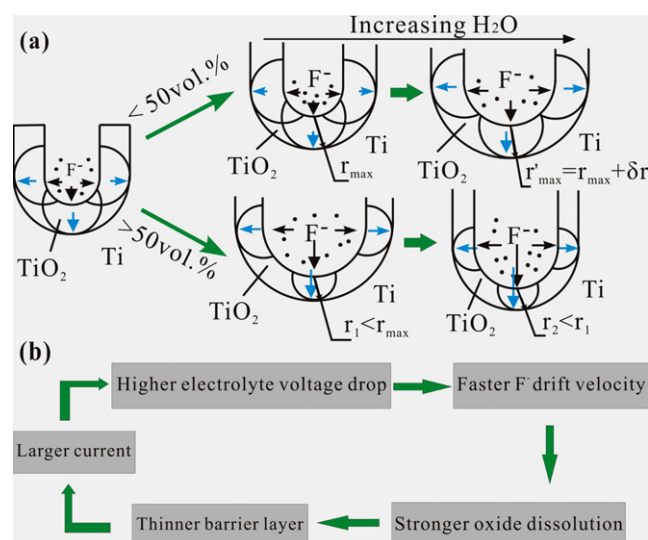


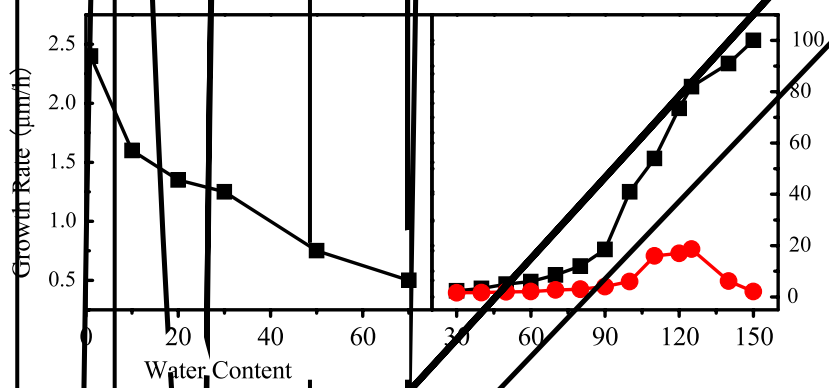
**Figure 3.** (a) Schematic illustration of the mechanism of  $\text{TiO}_2$  tube formation: the diameter changing with the increasing water concentration. Black and blue arrows indicate dissolution and oxidation processes, respectively. (b) High speed growth mechanism for  $\text{TiO}_2$  nanotube formation by stable high field anodization.

the top of the tube due to the highly concentrated and mobile  $\text{F}^-$  ions. Compared to the low voltage counterpart, the high voltage limit drops much faster since the dissolution is more affected by the increasing  $\text{H}_2\text{O}$  content at high field. Therefore, the voltage range in which ordered  $\text{TiO}_2$  nanotubes can be formed shrinks as the water content increases.

### 3.3. Optimizing the growth rate

Figure 4(a) shows the growth rate of the anodic  $\text{TiO}_2$  nanotube arrays at 30 V in 0.09 M  $\text{NH}_4\text{F}$  in EG with different water contents. It is clear that the growth rate decreases significantly with the increasing water concentration in the electrolyte. With the increase of the water concentration, the mobility of  $\text{H}^+$  and  $\text{F}^-$  is increased, and so is the concentration of  $\text{F}^-$ , as mentioned in section 3.2, which induces a significant increase in chemical dissolution at the top of the nanotube. Despite the dissolution at the tube bottom also being accelerated [10], resulting in a growth of the tube tip, the dissolution of the top increases much faster than the tip growth. As a result, the overall growth rate, which depends on both the dissolution at the top of the tube and the growth at the bottom [28], decreases with the increasing water content.

The growth rate is also inseparably linked with the total transferred charge per unit time [28]. Figure 5 presents the relationship between the  $\text{TiO}_2$  tube length for a constant growth time and the total transferred charge ( $\int I dt$ ) for different anodization voltages and water concentrations. It should be noticed that at the same water concentration, the data at the different voltages fall on the same straight line, i.e., the tube length is linearly proportional to the total charge transferred in a given time, where the larger quantity of total transferred charge is obtained at the higher voltage. Therefore, increasing the applied voltage is an especially efficient way to achieve



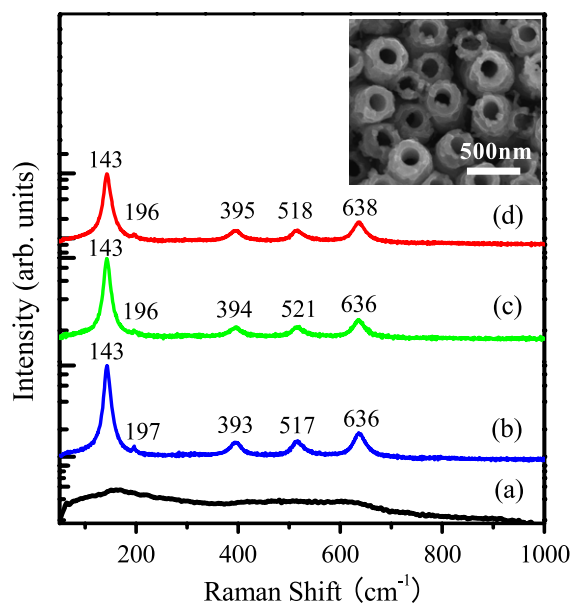


**Figure 6.** Raman spectra of (a) as-prepared and ((b)–(d)) annealed  $\text{TiO}_2$  nanotube arrays. The samples in (a) and (b) were obtained at 90 V in electrolyte with 10 vol%  $\text{H}_2\text{O}$ , while those in (c) (with the largest diameter of  $\sim 600$  nm) and (d) (with the highest growth rate of  $\sim 100 \mu\text{m h}^{-1}$ ) were fabricated at 150 V in electrolyte with 10 and 1 vol%  $\text{H}_2\text{O}$ , respectively. The annealing was carried out in air for 10 min at  $500^\circ\text{C}$ . The Raman peaks exhibited at 143, 196–197, 393–395, 517–521, and 636–638  $\text{cm}^{-1}$  demonstrate the formation of anatase  $\text{TiO}_2$  after annealing. The inset shows the SEM image taken from the annealed largest tube whose corresponding Raman spectrum is shown in (c).

DSSCs [3], biomedicine [6], and so on. Thermal annealing is a convenient way to obtain crystalline formation of the anodized  $\text{TiO}_2$  nanotube arrays with the well-ordered tubular structure retained [29, 30]. Figure 6 presents the room temperature Raman spectra of (a) as-prepared  $\text{TiO}_2$  nanotube arrays and ((b)–(d)) annealed ones, with the annealing carried out in air for 10 min at  $500^\circ\text{C}$  with the heating rate of  $10^\circ\text{C min}^{-1}$ . The thermal stability of the tubes is demonstrated by the inset SEM image taken from the annealed largest tube whose Raman spectrum is shown in figure 6(c). A broad Raman spectrum is shown by in curve (a), indicating that the as-prepared  $\text{TiO}_2$  is amorphous. In contrast, the annealed  $\text{TiO}_2$  nanotubes (curve (b)) exhibit specific Raman peaks at 143, 197, 393, 517, and 636  $\text{cm}^{-1}$ . It is well known that the structure of anatase  $\text{TiO}_2$  belongs to the space structure group of  $D_{4h}^{19} = I4_1/amd$ . It has six Raman active vibrational modes, with the corresponding peaks of 144  $\text{cm}^{-1}$  ( $E_g, \nu_6$ ), 197  $\text{cm}^{-1}$  ( $E_g, \nu_5$ ), 399  $\text{cm}^{-1}$  ( $B_{1g}, \nu_3$ ), 514  $\text{cm}^{-1}$  ( $A_{1g} + B_{1g}, \nu_1 + \nu_2$ ), and 639  $\text{cm}^{-1}$  ( $E_g, \nu_4$ ) [31]. We have further annealed the  $\text{TiO}_2$  nanotubes with the largest diameter of  $\sim 600$  nm and with the highest growth rate of  $\sim 100 \mu\text{m h}^{-1}$ , which were fabricated at 150 V in electrolyte with 10 and 1 vol%  $\text{H}_2\text{O}$ , respectively. The corresponding Raman results, curves (c) and (d), display similar peaks to curve (b). It is clear that our Raman observation has unambiguously demonstrated the successful transformation of amorphous  $\text{TiO}_2$  into anatase  $\text{TiO}_2$  nanotube arrays after thermal annealing, including the extreme specification ones.

## 4. Conclusions

In summary, we have developed a simple and efficient way to tune the diameter (50–600 nm) and optimize the growth rate (up to  $\sim 100 \mu\text{m h}^{-1}$ ) of the self-organized  $\text{TiO}_2$  nanotube arrays in electrolytes consisting of water, ethylene glycol, and ammonium fluoride. A complete phase diagram of the nanotube formation at room temperature has been established through a systematic investigation over a wide range of water concentration (1–100 vol%) and voltage (10–150 V). We have found that the nanotube diameter increases with the water concentration up to 50 vol%, while the growth rate decreases monotonically with the increasing water content. The diameter varies directly with the voltage applied in the electrolyte, and the growth rate soars in the high field. However, the anodization voltage range in which ordered nanotubes can be formed shrinks significantly as the water concentration increases. The success of the present work lies in the clear understanding of the effects of both the water content and anodization voltage on the formation of  $\text{TiO}_2$  nanotube arrays. In addition, we have converted all the as-prepared amorphous  $\text{TiO}_2$  nanotube arrays into anatase phase by annealing at high temperature in air. The mechanisms of the water content effect on the diameter and growth rate clarified in this study should provide tools for further optimization of the  $\text{TiO}_2$  nanotubes under different electrolyte compositions and temperatures. Moreover, the idea advanced in the present work will also provide a wide range for tuning the geometries of tube or pore nanostructures of other anodization valve metals, such as Zr and Hf.

## Acknowledgments

This work was supported by the Natural Science Foundation of China (contract No. 10734020), the National Major Basic Research Project of 2010CB933702, and Shanghai Municipal Commission of Science and Technology Project of 08XD14022. The authors would like to acknowledge technical assistance from Drs G Q Ding and Y F Zhu.

## References

- [1] Fujishima A and Honda K 1972 *Nature* **238** 37
- [2] O'Regan B and Gratzel M 1991 *Nature* **353** 737
- [3] Mor G K, Shandar K, Paulose M, Varghese O K and Grimes C A 2006 *Nano Lett.* **6** 215
- [4] Albu S P, Ghicov A, Macak J M and Schmuki P 2007 *Nano Lett.* **7** 1286
- [5] Kitao M, Oshima Y and Urabe K 1997 *Japan. J. Appl. Phys.* **1** **36** 4423
- [6] Tsuchiya H, Macak J M, Muller L, Kunze J, Muller F, Greil P, Virtanen S and Schmuki P 2006 *J. Biomed. Mater. Res. A* **77A** 534
- [7] Shinsuke Y, Tsuyoshi H, Hiroaki M, Ken K and Masayoshi U 2004 *J. Alloys Compounds* **373** 312
- [8] Hsin H O and Shang L L 2007 *Sep. Purif. Technol.* **58** 179
- [9] Bavykin D V, Friedrich J M and Walsh F C 2006 *Adv. Mater.* **18** 2807
- [10] Macak J M and Schmuki P 2006 *Electrochim. Acta* **52** 1258
- [11] Macak J M, Tsuchiya H, Tavera L, Aldabergerova A and Schmuki P 2005 *Angew. Chem. Int. Edn* **44** 7463
- [12] Wang J and Lin Z Q 2008 *Chem. Mater.* **20** 1257

- [13] Prakasam H E, Shankar K, Paulose M, Varghese O K and Grimes C A 2007 *J. Phys. Chem. C* **111** 7235
- [14] Zwilling V, Darque-Ceretti E, Boutry-Forveille A, David D, Perrin M Y and Aucouturier M 1999 *Surf. Interface Anal.* **27** 629
- [15] Gong D, Grimes C A, Varghese O K, Hu W, Singh R S, Chen Z and Dickey E C 2001 *J. Mater. Res.* **16** 3331
- [16] Mor G K, Varghese O K, Paulose M, Mukherjee N and Grimes C A 2003 *J. Mater. Res.* **18** 2588
- [17] Macak J M, Tsuchiya H and Schmuki P 2005 *Angew. Chem. Int. Edn* **44** 2100
- [18] Albu S P, Ghicov A, Macak J M and Schmuki P 2007 *Phys. Status Solidi (RRL)* **1** R65
- [19] Paulose M, Shankar K, Yoriya S, Prakasam H E, Varghese O K, Mor G K, Latempa T A, Fitzgerald A and Grimes C A 2006 *J. Phys. Chem. B* **110** 16179
- [20] Macak J M, Zlamal M, Krysa J and Schmuki P 2007 *Small* **3** 300
- [21] Valota A, LeClere D J, Skeldon P, Curioni M, Hashimoto T, Berger S, Kunze J, Schmuki P and Thompson G E 2009 *Electrochim. Acta* **54** 4321
- [22] Macak J M, Hildebrand H, Marten-Fahns U and Schmuki P 2008 *J. Electroanal. Chem.* **621** 254
- [23] Paulose M, Prakasam H E, Varghese O K, Peng L, Popat K C, Mor G K, Desai T A and Grimes C A 2007 *J. Phys. Chem. C* **111** 14992
- [24] Wang D A, Liu Y, Yu B, Zhou F and Liu W M 2009 *Chem. Mater.* **21** 1198
- [25] Balaur E, Macak J M, Tsuchiya H and Schmuki P 2005 *J. Mater. Chem.* **15** 4488
- [26] Grimes C A and Mor G K 2009 *TiO<sub>2</sub> Nanotube Arrays Synthesis, Properties and Applications* (New York: Springer) p 318
- [27] Ghicov A and Schmuki P 2009 *Chem. Commun.* **20** 2791
- [28] Yasuda K and Schmuki P 2007 *Electrochim. Acta* **52** 4053
- [29] Wang J and Lin Z Q 2009 *J. Phys. Chem. C* **113** 4026
- [30] Albu S P, Ghicov A, Aldabergenova S, Drechsel P, LeClere D, Thompson G E, Macak J M and Schmuki P 2008 *Adv. Mater.* **20** 4135
- [31] Ohsaka T, Izumi F and Fujiki Y 1978 *J. Raman Spectrosc.* **7** 321